Influence of current density and inlet gas flow in the treatment of gaseous streams polluted with benzene by electro-absorption

Andrea N. Arias, Rafael Granados-Fernández, C.M. Fernández-Marchante*, J. Lobato, Manuel A. Rodrigo

Department of Chemical Engineering, Faculty of Chemical Sciences & Technologies, Universidad de Castilla - La Mancha, Campus Universitario s/n, 13071 Ciudad Real, Spain

Abstract

This paper is focused on the evaluation of the electrochemically assisted absorption process (electro-absorption) as a treatment for volatile organic compounds contained in polluted air flows. Benzene degradation was used to test the technology, using a system consisting of a packed absorption column and a single compartment electrochemical cell equipped with boron-doped diamond (BDD) as anode and steel-steal as cathode. The influence of inlet gas flow rate and operation current intensity was evaluated by monitoring the concentration of benzene and intermediates both, in the liquid absorbent / electrolyte and in the outlet gaseous stream. Results show that steady-state values reached, during benzene absorption and electro-absorption, increase when the inlet gas flow rises from 1.5 to 6.0 L h^{-1} and that the bare absorption process retains benzene only up to this steady-state value of the liquid and then, it has no effect on the removal of benzene. Concentrations of benzene in the absorbent/electrolyte decreases with the increase in the current density during electrochemically assisted processes. As well, mineralization was found to be very important, as expected because of the very low concentrations of benzene into the liquid and the very

high efficiencies of the electrolytic degradation with BDD electrodes, and benzoquinone and carboxylic acids were identified as the primary intermediates. These species were not detected in the outlet gas flow. The decrease in the concentration and mass flow of benzene in the outlet streams confirms that electro-absorption is a functional electrochemical application to remove benzene from gaseous streams. When current density rises (10, 50 and 100 mA cm^{-2}), the degradation percentage increases. The values obtained were 43, 61 and 75 % with 1,5 L h^{-1} of inlet gas flow and 10, 25 and 37 % with 6 L h^{-1}. However, the degradation percentage relative to the energy consumption decreases when the current density rises. Results were, correspondingly, 24.7, 4.2 and 2.2 % kWh^{-1} with 1,5 L h^{-1} of inlet gas flow and 7.1, 2.1 and 1.4 % with 6 L h^{-1}. This energy efficiency trend was explained because mass transport becomes the bottleneck in the oxidation of diluted organic solutions. These results contribute to expand the understanding of the mechanisms involved in the electro-absorption of benzene and recommend for further research in the topic, due to the relevance of the treatment results.

Keywords

Electro-absorption, benzene, boron-doped diamond, current density, inlet gas flow.

Highlights

- Efficient mineralization of the VOCs contained in the air using electro-scrubbing technology.
- Benzoquinone and carboxylic acids are formed in the absorbent but not found in the outlet stream.

- Percentage of benzene gaseous removal increases by increasing operation current density.
- Mass transport control of the electrochemical degradation of benzene into the absorbent/electrolyte.

Graphical Abstract

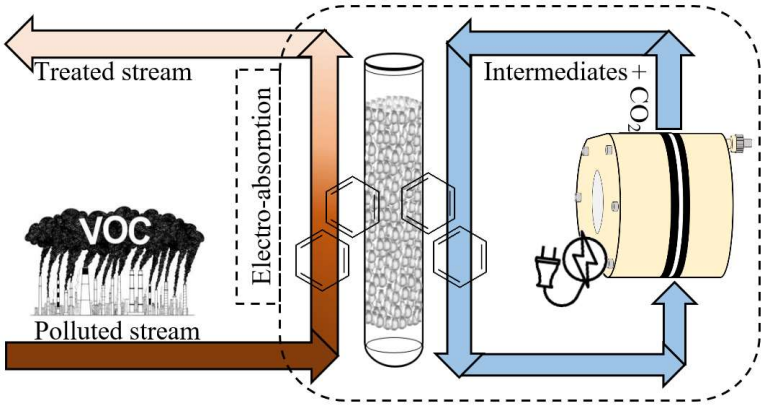

*Corresponding author

E-mail address: carmenm.fmarchante@uclm.es (C.M. Fernández-Marchante)

1. Introduction

In the last decades, volatile organic compounds (VOCs) had constituted a relevant group of chemicals used in different processes in several industries, such as paints and solvents [1], rubbers [2], wooden furniture [3], anode manufacturing [4], polyester fabric [5] and asphalt pavement [6], among many others. These activities are associated with an environmental problem that is becoming of major relevance: the generation of gaseous polluted streams [7] which influence not only human health but also air quality and tropospheric chemistry [8]. Nowadays, VOCs contained in polluted air are mainly destroyed by different oxidation processes including thermal, catalytic, and biological [9–11].

In recent years, very efficient electrochemical applications have been developed to treat liquid wastes and it has been pointed out the high impact of the choice of the anodic material [12–15] and operation conditions on the performance attained [16–20]. These interesting results have pushed researchers to expand the scope to the treatment of gaseous pollutants. An innovative technology is electro-absorption (also called electro-scrubbing). It combines physical or chemical absorption and electro-oxidation. The first step allows the molecules of the pollutant to transport from the gaseous to the bulk of the liquid phase. Principal parameters to consider are the type of packing, column dimensions, transfer coefficients and feed flowrates [21]. The second step is carried out in an electrochemical cell and enables the elimination of the pollutants by the oxidation reactions which can take place on the surface of the electrodes and/or in the liquid bulk by the oxidants produced. Important parameters in electro-oxidation are electrodes material, electrolyte, current density and cell voltage [22–25]. This process is now developed at technology readiness levels (TRL) of 3-4, and the interest has been mainly focused on the removal of VOCs and odour substances [26–30] but applicability may be extended also to atmospheric pollutants. Hence, there is a great need for

81 further research up to meet an industrial TRL of 7-9, and in the incoming years many
82 scientific and technically sound works are expected on this topic. Some advantages of
83 electro-absorption as compared to in-use technologies are the high efficiency of anodic
84 oxidation, the regeneration of the absorbent solution, the possibility of optimizing the
85 formulation of the absorbent and the fact that the primary reagents used are the electrons.
86 Considering this background, this study aims to evaluate the electro-scrubbing of streams of
87 air polluted with benzene, where this species has been used as a model of VOC. Packed
88 absorption column and single compartment electrochemical cell are combined using anode
89 consisting of boron-doped diamond and the effect of the current densities for two different
90 feeding flowrates has been clarified, paying attention to the intermediates formed and the
91 decrease of benzene concentration in the polluted gas stream after the application of the
92 electro-absorption process.
93
94 **2. Experimental**
95 **2.1 Chemicals**
96 All the chemical reagents were used as received and were analytical grade. The main ones
97 were benzene 99.9% (Sigma-Aldrich), sulfuric acid 97% and hexane HPLC grade (Scharlau).
98 Also, the following potential intermediates and by-products typically reported in the
99 oxidation of benzene [31–34] were used: benzoquinone 98% (Panreac), phenol 99% (Sigma-
100 Aldrich), maleic acid 99% (Panreac), malonic acid 99% (Sigma-Aldrich), acetic acid 96%
101 (Panreac), formic acid 98% (Sigma-Aldrich) and oxalic acid 99% (Sigma-Aldrich). All
102 solutions were prepared with deionized water (Millipore Mili-Q system, resistivity 18.2 MΩ
103 cm at 25°C). Helium (Al Air Liquide España), filtered by a hydrocarbon cartridge filter

(Thermo Fisher Scientific), was used for the gas chromatography. Active carbon was BD CARBON GR 10.3 (Barcelonesa).

2.2 Experimental setup and procedure

A commercial electrochemical cell (DiaCell, purchased to Adamant Technologies, France) and a packed absorption column were integrated to constitute the electrochemically assisted absorption system shown in Figure 1 (electro-absorber). The column was made of glass with an inner diameter of 0.05 m, length of 0.5 m, and a packing height of 0.4 m, and it was filled with glass spheres (8 mm diameter) randomly distributed. A synthetic polluted gaseous stream was obtained by bubbling air (1) [35] into a tank filled with liquid benzene (99,9%) (3). The gas flowrate was monitored with a rotameter (2) and the inlet of the gas was placed in the bottom of the absorption column (4). The absorbent liquid was contained in a tank (1L, 0.05 M H_2SO_4), from which it was pumped to the top of the column by a peristaltic pump (8) with a flow (10 L h^{-1}) monitored with a rotameter (9). Both streams had countercurrent contact (7). The liquid stream that comes out from the bottom of the column went to a single-compartment electrochemical flow cell (5). The anode is boron-doped diamond (BDD) with Si as support and the cathode is commercial stainless steel (SS), both having a circular shape with an area of 78 cm^2. The distance between the electrodes is 5 mm. A power supply (6) provides a constant intensity to the cell during each of the tests carried out. The liquid stream that comes from the cell was recirculated to the reactor tank, while its gaseous stream and the outlet gas from the column were mixed and conducted to an active carbon column to retain unreacted benzene and intermediates from the system. In this way, it can be considered that the gaseous phase performs in continuous mode (red line) while the liquid phase works in batch mode (blue line).

The flowrates of gas treated evaluated were 1.5 and 6.0 L h^{-1} and current densities applied were 10, 50 and 100 mA cm^{-2}. Absorption corresponds to experimentation with 0 mA cm^{-2}. Each experimental test was carried out with a new electrolyte solution.

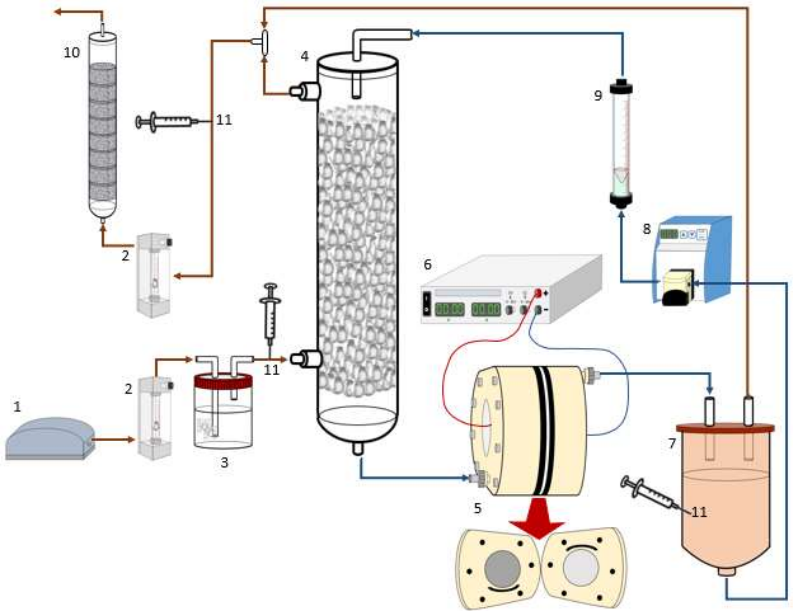

Figure 1. Electro-absorber installation scheme. (1) air compressor, (2) rotameter, (3) liquid benzene tank, (4) packed absorption column, (5) flow electrochemical cell with BDD as anode and stainless steel as cathode, (6) power supply, (7) reactor tank, (8) peristaltic pump, (9) flow meter, (10) active carbon column, (11) sampling points.

2.3 Analytical techniques

From the reactor tank, liquid samples were collected (2.0 mL). They underwent L-L extraction with hexane (6 mL) in a vortex stirrer for 2 minutes. After the two phases were split, hexane was transferred to a gas chromatography (GC) vial. From the absorption column and the activated carbon column inlets, gaseous samples (5.0 mL) were taken and bubbled directly in hexane (10.0 mL). Then, they were collected in a GC vial. Compound

concentrations in the samples were measured by Shimadzu Gas Chromatography (Nexis GC-2030) coupled to a Mass Spectrometer Detector (GCMS-QP2020 NX). The capillary analytical column was a SH-Rxi-5Ms 30m x 0.25 mm x 0.25um with a split/splitless injector in split mode (ratio of 20) and a total flow of 42.8 mL min^{-1} (pressure 100.0 kPa) with a linear velocity of 48.3 cm s^{-1}. Temperature column program was: 38.0 ºC for 3 min, 40.0 ºC min^{-1} to 75.0 ºC and 30.0 ºC min^{-1} to 200.0 ºC for 2 min. The injection and detector temperatures were 200.0 ºC. The carboxylic acids were measured by HPLC with a Hi-Plex H column (Agilent Technologies) and a 5.0 mM sulfuric acid aqueous solution as the mobile phase (0.8 mL min^{-1}). The wavelength was 210 nm. Total organic carbon (TOC) was measured by Multi N/C 3100 analyser (Analytik Jena).

3. Results and Discussion

Figure 2 shows the concentration and mass flow of benzene fed into the absorption (0 mA cm-2) and electro-absorption processes, in which the effect of the carrier flowrate (1.5 and 6.0 L h^{-1}) and operating current densities (10, 50 and 100 mA cm^{-2}) were evaluated. Obviously, the inlet is not influenced by the treatment applied, although it gives relevant information about the variability of the inputs in this experimental device. Thus, as it can be observed, there is a fluctuation of nearly 15% in the inlet measurements (188 ± 28 mg C L^{-1}), that can be explained in terms of the high turbulence produced by the bubbling of air in the benzene tank. This dispersion is also observed in the mass flow fed and the average values were 4.23 ± 0.63 and 19.21 ± 2.02 mg C min^{-1} at 1.5 and 6 L h^{-1} respectively.

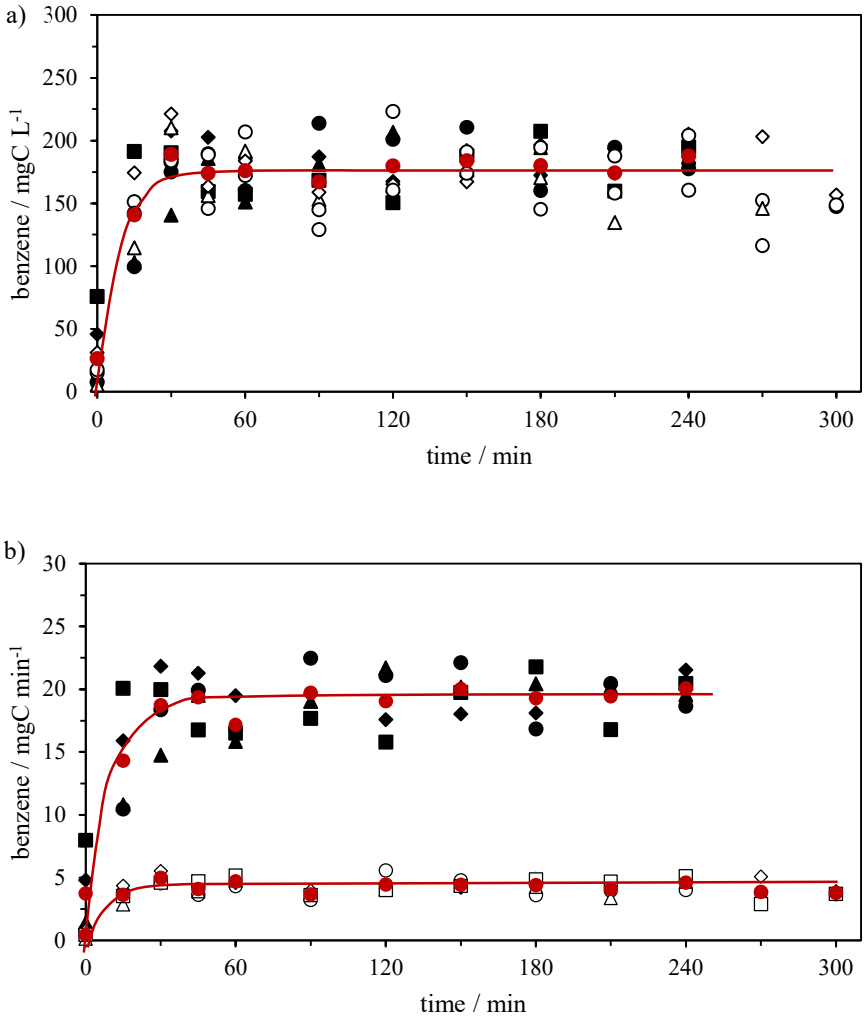

Figure 2. Time evolution of benzene a) concentration and b) mass flow in inlet gaseous flow of 1.5 (white) and 6 (black) L h^{-1}. Averages of every time (red points) and their trend line (red line). Absorption (circle) and electro-absorption processes at 10 (triangle), 50 (rhombus) and 100 (square) mA cm^{-2}.

Figure 3 shows the time course of the benzene concentration in the absorbent liquid phase during the absorption and electro-absorption tests. Regarding the non-electrochemical process, as expected, only benzene is measured in the liquid and no reactivity is associated. This is because of the low reactivity of VOCs under absorption conditions. A similar behavior

was observed in the degradation of toluene [26]. Physical adsorption of benzene in water is not affected by the concentration of the electrolyte used (0.05 M H_2SO_4) [36]. It mainly depends on equilibrium (and hence on the temperature and pressure) and mass transport (where flowrates are expected to influence). Thus, since temperature and pressure were kept constant during the tests (25ºC and 93 kPa), the latest justifies that the amount of benzene absorbed by the system grows by increasing the gas inlet flow (mass flow). Steady-state value was around three times lower in the absorbent of the system fed with 1.5 than with 6.0 L h^{-1} of benzene polluted air, being the values in which the concentration stabilizes of 392.12 ± 16.01 and 1080.04 ± 51.48 mg C L^{-1}, respectively. Additionally, it can be observed that the concentration in the liquid reached a plateau after about three hours of feeding with 1.5 L h^{-1} of benzene polluted air and only one hour and a half of feeding the system with 6.0 L h^{-1}. More interesting are the stabilization concentrations reached in the electro-absorption, that is, when current is applied in the electrochemical cell connected to the absorption column: the benzene concentration achieved at steady-state in the liquid phase decreases with the increase in the current density. With a flow of 1.5 L h^{-1}, the values are 221.90 ± 7.79, 140.75 ± 8.85 and 46.40 ± 1.30 mg C L^{-1} in the electro-absorptions at current densities of 10, 50 and 100 mA cm^{-2}, respectively. In the tests in which the treatment technology is fed with 6.0 L h^{-1}, the concentrations reached with the same current density values were 829.06 ± 47.42, 690.02 ± 14.64 and 430.23 ± 22.38 mg C L^{-1}. When these values are compared with the obtained in the bare absorption, it is observed higher percentages of reduction in the lowest inlet gas flow tested. Thus, reduction values were 43.41, 64.11 and 88.17 % with 10, 50 and 100 mA cm-2. On the other hand, the tests with the highest inlet gas flowrate achieved a 23.24, 36.11 and 60.17 % of reduction in the stabilization concentration for the three increasing current densities tested in this work. This could happen because while the current

density increments, the production rate of oxidants increases as well. Consequently, as there is a greater amount of these reactants, the kinetics of benzene degradation in the liquid phase is higher and its steady-state value is lower. Additionally, it can be concluded that with an increase of four times in the inlet gas flow rate, the percentage of reduction in the steady-state concentration in the liquid phase is reduced from 1.5 to 1.9 times for the same value of current density.

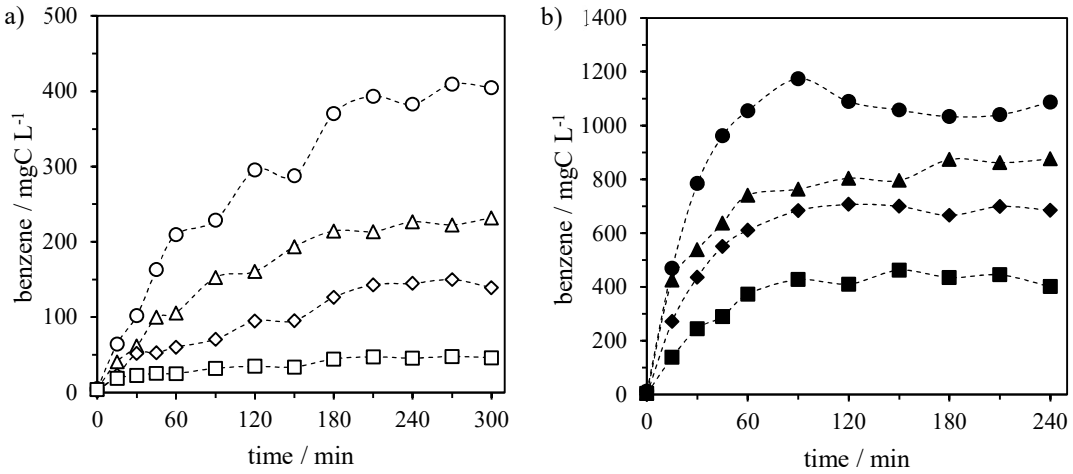

Figure 3. Time evolution of benzene concentration in liquid phase in absorption (circle) and electro-absorption processes at 10 (triangle), 50 (rhombus) and 100 (square) mA cm^{-2}. At different inlet gas flows of a) 1.5 (white) and b) 6 (black) L h^{-1}.

Figure 4 shows the time course of the total concentration of the intermediate compounds identified analytically in the liquid phase in electro-absorption processes at inlet gas flows of 1.5 and 6.0 L h^{-1}. The time evolution of each compound is in Figure S1. In both flow rates, benzoquinone was the principal aromatic intermediate identified, which reached maximum concentrations of 8.0 and 44.0 mg C L^{-1} for each inlet gas flow fed, respectively.

Additionally, carboxylic acids identified were oxalic, maleic, malonic and acetic. The concentration of the first one is higher when the current density increases, and the same behaviour happens with malonic acid. On the other hand, the other acids show the highest concentration at 10 mA cm^{-2}, while at 50 and 100 mA cm^{-2} their concentrations are much smaller. In the tests with 1.5 L h^{-1} of inlet gas flow, all maximum concentrations of carboxylic acids are lower than 10 mg C L^{-1}, while with 6 L h^{-1} they do not exceed 40 mg C L^{-1}. The carbon mass of the intermediates represents less than 10% of the total mass that enters in the system in both inlet gas flows. So, this fact could infer that there is not an accumulation of intermediates and mineralization is the principal way of the benzene electro-degradation process. Also, these results help to have information about the degradation route of benzene which could consist first in the oxidation of the aromatic ring before its breakup and subsequent formation of carboxylic acids to finally reach mineralization. This statement is in concordance with other authors [37–40].

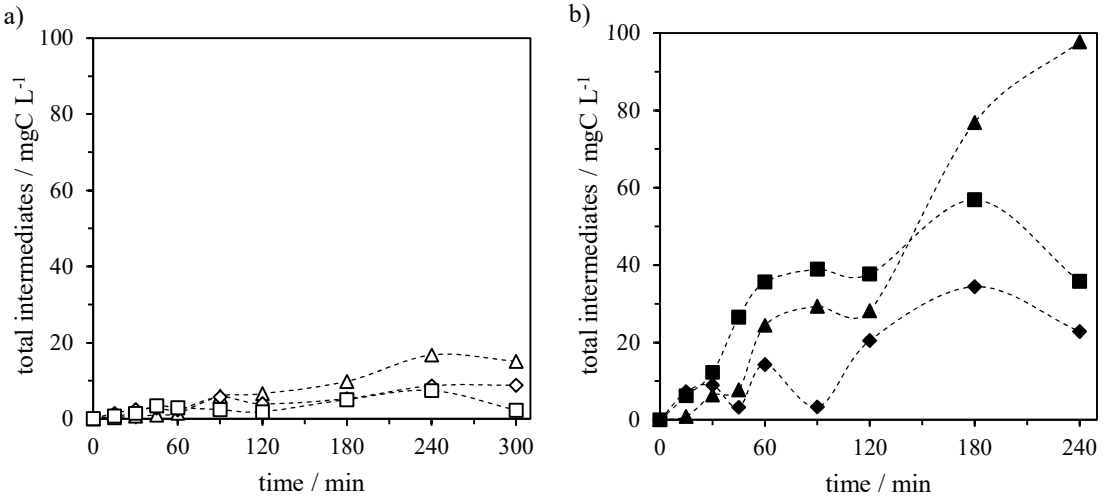

Figure 4. Time evolution of the total concentration of intermediate compounds identified in the liquid phase at a gaseous flow of a) 1.5 (white) and b) 6 (black) L h^{-1} in electro-absorption processes at 10 (triangle), 50 (rhombus) and 100 (square) mA cm^{-2}

Total organic carbon (TOC) was calculated by the sum of benzene and intermediates compounds concentrations, and it is compared with TOC measured analytically, results are shown in Figure 5. It is observed that theoretical and measured TOC values have a good fitting coefficient (R^2 0.97). This means that the mass of carbon missed from the input value is mineralized and that there are no other relevant intermediates unidentified that are interfering with TOC measurement.

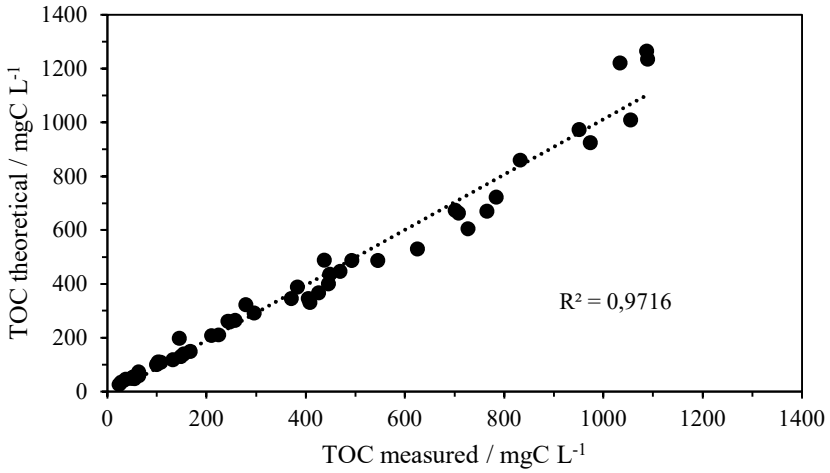

Figure 5. TOC theoretical vs measured in liquid phase in absorption and electro-absorption processes at 10, 50 and 100 mA cm^{-2} at different inlet gas flow of 1.5 and 6.0 L h^{-1}.

Values shown in figures 3 to 5 are important to understand the performance of the electro-absorption technology. However, the most important information comes from the comparison of the concentrations and mass flow of benzene in the gaseous outlet streams.

Figure 6 shows the concentration of benzenes detected in this stream during the different tests and Figure 7 collects the mass flow of outlet gas in absorption and electro-absorption tests at gas flow rates of 1.5 and 6.0 L h^{-1}. The first Figure confirms that concentrations of benzene in the treated gas reach a steady-state value in less than three hours, which corresponds to the same concentration of the inlet (Figure 2) in the case of the bare absorption technology (as expected, because of the steady-state value reached in the absorbent capacity) and too much lower values in the concentration of benzene in the outlet gas of the electro-absorbers when the electric current is applied, as explained because of the electrochemical destruction of benzene and formation of intermediates.

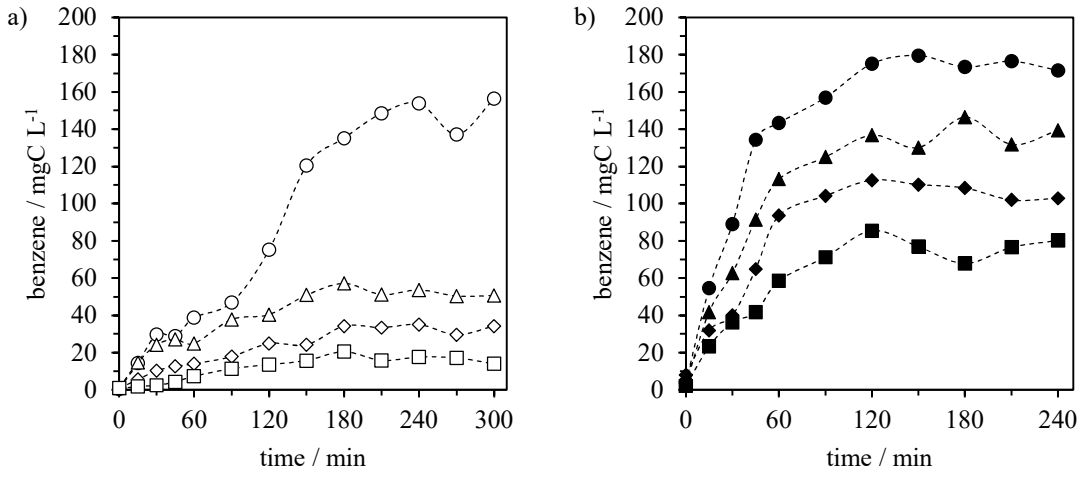

Figure 6. Time evolution of benzene concentration in outlet gas flow in absorption (circle) and electro-absorption processes at 10 (triangle), 50 (rhombus) and 100 (square) mA cm^{-2}. At different inlet gas flows of a) 1.5 (white) and b) 6 (black) L h^{-1}.

The decrease in benzene concentrations in the outlet gas is also reflected in the observed differences in the mass flow rate escaping treatment (Figure 7). Thus, it is observed that when absorption is carried out, the benzene concentration gradually increases until the input value

is reached. This fact means that liquid is no longer able to absorb benzene and, this phenomenon happens about three hours with the 1.5 L h^{-1} flow rate and one hour and a half with 6.0 L h^{-1}. It could be explained because the equilibrium concentration between liquid and gaseous phases strongly depends on the partial pressure, mass flow in other words, of the target compound within the gas phase in absorption. In addition, increasing the gas flow induces more turbulence inside the column that leads to better interface contact between the liquid and gas phases improving the mass transfer rate. However, the higher the gas flow, the shorter is the residence time of the gas in the system, which affects the diffusivity of the pollutant [41]. So, it is important to find an optimal point between these parameters. The steady-state flow was 4.02 ± 0.26 and 18.94 ± 0.87 mg C min^{-1} and the difference in percentage in relation with the inlet mass flow was 2.20 and 3.56 % respectively with 1.5 and 6.0 L h^{-1} of inlet gas flow rate.

Regarding the electro-absorption tests, it is clearly observed that the higher is the current density, the lower is the mass flow value that the outlet gas reaches in the steady-state. With a flowrate of polluted air of 1.5 L h^{-1} and current densities of 10, 50 and 100 mA cm^{-2}, the outlet gas mass flows were 1.58 ± 0.09, 1.17 ± 0.08 and 0.68 ± 0.10 mg C min^{-1} respectively. Meanwhile, with 6.0 L h^{-1}, these values are 15.52 ± 0.87, 13.34 ± 0.54 and 10.70 ± 0.88 mg C min^{-1}. When these results are compared with the inlet mass flow in each test at different current densities, the reduction percentages are 61.53, 73.64 and 84.09 % with the lowest inlet gas flow and 18.48, 32.50 and 41.86 % with the highest one. In a similar way to the liquid phase, it can be determined that with an increase of four times in the inlet gas flow rate, the percentage of reduction in the steady-state concentration in the outlet gas mass flow is reduced from 2.0 to 3.3 times for the same value of current density.

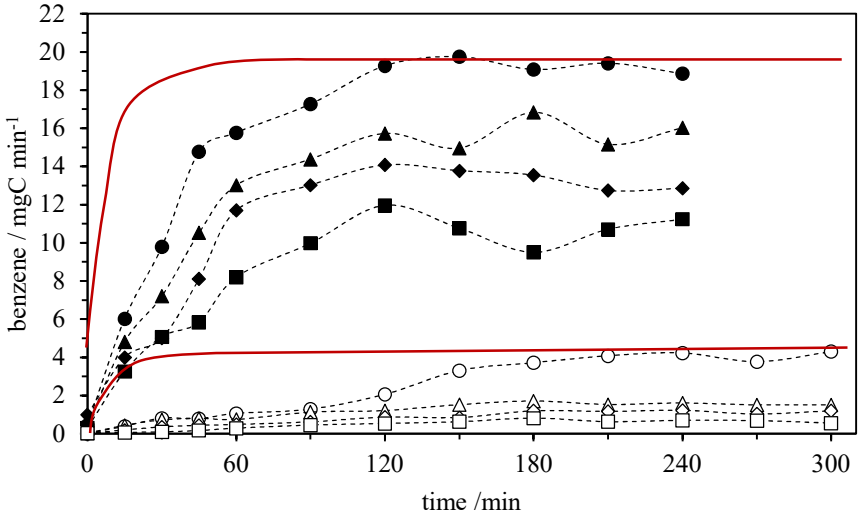

Figure 7. Time evolution of benzene mass flow in outlet gas stream in absorption (circle) and electro-absorption processes at 10 (triangle), 50 (rhombus) and 100 (square) mA cm^{-2}. At different inlet gas flows of a) 1.5 (white) and b) 6.0 (black) L h^{-1}. Mass flow of benzene in the inlet gas (red line in Figure 2b).

The mass of benzene adsorbed in the active carbon column which represents the amount not treated is shown in Table S1. In addition, no intermediates were identified in the gases outflowing from the system, which can be explained by the very low concentrations measured in the absorbent liquids and, also, by the very low volatility of all the intermediates. This supports the technical feasibility of the treatment proposed for these gases containing VOCs as has been demonstrated with other compounds [24,42–44]. As well, energy and efficiency considerations are important to be discussed and this information is provided in Figure 8, where Part a indicates that the degradation percentage rises with current density and Part b, which represents the degradation percentage relative to kWh (calculated with the

voltage, intensity and total time of each test) that energy efficiency decreases very importantly with current density. This lower efficiency at higher current densities is expected because of the mass transport control of the electrochemical process in liquid phase which, in turn, can be associated to the low concentration of pollutants.

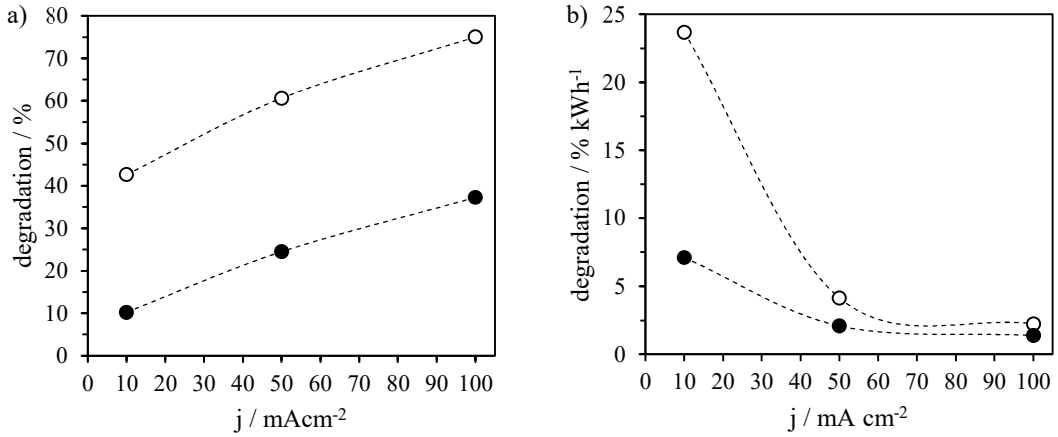

Figure 8. Degradation percentage a) absolute and b) relative to kWh at different current densities. Inlet gaseous flow of 1.5 (white) and 6.0 (black) L h^{-1}.

CONCLUSIONS

Conclusions obtained in this study are the following:

- Electrochemically assisted absorption processes are efficient in the degradation of benzene contained in polluted air and may become a very interesting choice if the TRL increases. Positive results obtained in this work are promising a recommend further work in the topic.
- Polluted air can be simulated by bubbling air into liquid benzene. Inlet gas concentration is constant and independent of the gas flow rate, in contrast to the mass flow which is proportional with this parameter. Additionally, steady-state

concentration of benzene absorbed increases and is reached in half the time when inlet gas flow rises from 1.5 to 6.0 L h^{-1}.

- Intermediates compounds identified during electro-absorption processes are benzoquinones and carboxylic acids such as oxalic, maleic, malonic and acetic. Their concentration is very low, as expected for an electrochemical oxidation of organics with boron-doped diamond electrodes. Therefore, mineralization is considered the primary degradation mechanisms of benzene in electro-absorption process.
- Electro-absorption process is functional to the treatment of gaseous streams polluted with benzene, a higher percentage of benzene removal from the gaseous stream is obtained by increasing the current density and decreasing the mass flow of inlet gas flow. The same behaviour is observed in the liquid phase.
- Degradation percentage relative to energy consumption increases when the current density decrease, this energy efficiency relation with current density is due to the limitations in mass transport control during the oxidation of diluted aqueous wastes.

Author contributions

Andrea N. Arias: Investigation, Data curation, Formal analysis, Writing – original draft. **R. Granados-Fernández**: Writing – review & editing. **J. Lobato**: Funding acquisition, Project administration, Supervision, Validation, Writing – review & editing. **Carmen M. Fernández-Marchante**: Supervision, Validation, Writing – review & editing. **Manuel A. Rodrigo**: Conceptualization, Funding acquisition, Project administration, Supervision, Validation, Writing – review & editing.

Declaration of competing interest

The authors declare that they have no known competing financial interests or personal relationships that could influence the work reported in this paper.

Acknowledgments

Financial support the Spanish Ministry of Economy, Industry and Competitiveness, European Union through project PID2019-107271RB-I00 (AEI/FEDER, UE) is gratefully acknowledged. Andrea N. Arias acknowledge the FPI grant nº PRE2020-094902.

References

[1] Z. Liu, Y. Yan, T. Lv, Z. Huang, T. Liu, Q. Huang, J. Yang, Y. Chen, Y. Zhao, T. Zhou, Comprehensive understanding the emission characteristics and kinetics of VOCs from automotive waste paint sludge in a environmental test chamber, Journal of Hazardous Materials. 429 (2022) 128387. https://doi.org/10.1016/j.jhazmat.2022.128387.

[2] N.F. Idris, N. Le-Minh, J.E. Hayes, R.M. Stuetz, Performance of wet scrubbers to remove VOCs from rubber emissions, Journal of Environmental Management. 305 (2022) 114426. https://doi.org/10.1016/j.jenvman.2021.114426.

[3] Y. Wang, H. Wang, Y. Tan, J. Liu, K. Wang, W. Ji, L. Sun, X. Yu, J. Zhao, B. Xu, J. Xiong, Measurement of the key parameters of VOC emissions from wooden furniture, and the impact of temperature, Atmospheric Environment. 259 (2021) 118510. https://doi.org/10.1016/j.atmosenv.2021.118510.

[4] S. Han, Q. Zhao, R. Zhang, Y. Liu, C. Li, Y. Zhang, Y. Li, S. Yin, Q. Yan, Emission characteristic and environmental impact of process-based VOCs from prebaked anode manufacturing industry in Zhengzhou, China, Atmospheric Pollution Research. 11 (2020) 67–77. https://doi.org/10.1016/j.apr.2019.09.016.

[5] W. Qian, Y. Guo, X. Wang, X. Qiu, X. Ji, L. Wang, Y. Li, Quantification and assessment of chemical footprint of VOCs in polyester fabric production, Journal of Cleaner Production. 339 (2022) 130628. https://doi.org/10.1016/j.jclepro.2022.130628.

[6] N. Li, Q. Jiang, F. Wang, J. Xie, Y. Li, J. Li, S. Wu, Emission behavior, environmental impact and priority-controlled pollutants assessment of volatile organic compounds (VOCs) during asphalt pavement construction based on laboratory experiment, Journal of Hazardous Materials. 398 (2020). https://doi.org/10.1016/j.jhazmat.2020.122904.

[7] B. McDonald, J. de Gouw, J. Gilman, S. Jathar, Volatile chemical products emerging as largest petrochemical source of urban organic emissions, Science. 764 (2018) 760–764.

[8] H. Lee, K. Kim, Y. Choi, D. Kim, Emissions of Volatile Organic Compounds (VOCs) from an Open-Circuit Dry Cleaning Machine Using a Petroleum-Based Organic Solvent : Implications for Impacts on Air Quality, (2021) 4–14.

[9] F.I. Khan, A.K. Ghoshal, Removal of Volatile Organic Compounds from polluted air, Journal of Loss Prevention in the Process Industries. 13 (2000) 527–545.

https://doi.org/10.1016/S0950-4230(00)00007-3.

[10] X. Li, Y. Niu, H. Su, Y. Qi, Simple Thermocatalytic Oxidation Degradation of VOCs, Catalysis Letters. (2021). https://doi.org/10.1007/s10562-021-03770-x.

[11] Y. Chu, J. Wang, G. Tian, R. He, Reduction in VOC emissions by intermittent aeration in bioreactor landfills with gas-water joint regulation ☆, Environmental Pollution. 290 (2021) 118059. https://doi.org/10.1016/j.envpol.2021.118059.

[12] K. Zhu, X. Wang, X. Ma, Z. Sun, X. Hu, Comparative degradation of atrazine by anodic oxidation at graphite and platinum electrodes and insights into electrochemical behavior of graphite anode, Electrocatalysis. 10 (2019) 35–44. https://doi.org/10.1007/s12678-018-0493-z.

[13] P. Zhu, Y. Shen, L. Dai, Q. Yu, Z.-M. Zhang, C. An, Accelerating anode reaction with electro-oxidation of alcohols over Ru nanoparticles to reduce the potential for water splitting, ACS Applied Materials and Interfaces. 14 (2022) 1452–1459. https://doi.org/10.1021/acsami.1c20511.

[14] A. Kurt, Cefuroxime Oxidation With New Generation Anodes: Evaluation Of Parameter Effects, Kinetic And Total Intermediate Products, Environmental Research and Technology. 4 (2021) 317–328. https://doi.org/10.35208/ert.867139.

[15] J. Carillo-Abad, J. Mora-Gómez, M. García-Gabaldón, E. Ortega, S. Mestre, V. Pérez-Herranz, Effect of the CuO addition on a Sb-doped SnO2 ceramic electrode applied to the removal of norfloxacin in chloride media by electro-oxidation, Chemosphere. 249 (2020) 1–9. https://doi.org/10.1016/j.chemosphere.2020.126178.

[16] C. Barrera-Díaz, P. Cañizares, F.J. Fernández, R. Natividad, M.A. Rodrigo, Electrochemical Advanced Oxidation Processes: An Overview of the Current Applications to Actual Industrial Effluents, Journal of the Mexican Chemical Society. 58 (2014) 256–275.

[17] C.A. Martínez-Huitle, M.A. Rodrigo, I. Sirés, O. Scialdone, Single and Coupled Electrochemical Processes and Reactors for the Abatement of Organic Water Pollutants: A Critical Review, Chemical Reviews. 115 (2015) 13362–13407. https://doi.org/10.1021/acs.chemrev.5b00361.

[18] M.A. Rodrigo, M.A. Oturan, N. Oturan, Electrochemically assisted remediation of pesticides in soils and water: A review, Chemical Reviews. 114 (2014) 8720–8745. https://doi.org/10.1021/cr500077e.

[19] I. Sirés, E. Brillas, M.A. Oturan, M.A. Rodrigo, M. Panizza, Electrochemical advanced oxidation processes: Today and tomorrow. A review, Environmental Science and Pollution Research. 21 (2014) 8336–8367. https://doi.org/10.1007/s11356-014-2783-1.

[20] W.C. Cho, K.M. Poo, H.O. Mohamed, T.N. Kim, Y.S. Kim, M.H. Hwang, D.W. Jung, K.J. Chae, Non-selective rapid electro-oxidation of persistent, refractory VOCs in industrial wastewater using a highly catalytic and dimensionally stable Ir–Pd/Ti composite electrode, Chemosphere. 206 (2018) 483–490. https://doi.org/10.1016/j.chemosphere.2018.05.060.

[21] M. Tokumura, R. Nakajima, H.T. Znad, Y. Kawase, Chemical absorption process for

428 degradation of VOC gas using heterogeneous gas-liquid photocatalytic oxidation:
429 Toluene degradation by photo-Fenton reaction, Chemosphere. 73 (2008) 768–775.
430 https://doi.org/10.1016/j.chemosphere.2008.06.021.

431 [22] F. Escalona-Duran, C. Saez, J. Lobato, C. Martínez-Huitle, M. Rodrigo,
432 Electroscrubbers for removing volatile organic compounds and odorous substances
433 from polluted gaseous streams, Current Opinion in Electrochemistry. 28 (2021).
434 https://doi.org/10.1016/j.coelec.2021.100718.

435 [23] P. Cañizares, C. Sáez, J. Lobato, R. Paz, M.A. Rodrigo, Effect of the Operating
436 Conditions on the Oxidation Mechanisms in Conductive-Diamond Electrolyses,
437 Journal of The Electrochemical Society. 154 (2007) E37.
438 https://doi.org/10.1149/1.2424409.

439 [24] M. Govindan, R. Adam Gopal, I.S. Moon, Efficient removal of gaseous
440 trichloroethylene by continuous feed electro-scrubbing using a new homogeneous
441 heterobimetallic electro-catalyst, Chemical Engineering Journal. 308 (2017) 1145–
442 1153. https://doi.org/10.1016/j.cej.2016.09.137.

443 [25] F. Escalona-Durán, M. Muñoz-Morales, C.M. Fernández-Marchante, J. Lobato, C.A.
444 Martínez-Huitle, M.A. Rodrigo, Modelling electro-scrubbers for removal of VOCs,
445 Separation and Purification Technology. 277 (2021).
446 https://doi.org/10.1016/j.seppur.2021.119419.

447 [26] M. Castañeda-Juárez, M. Muñoz-Morales, F.L. Souza, C. Sáez, P. Cañizares, P.T.
448 Almazán-Sánchez, I. Linares-Hernández, M.A. Rodrigo, Electro-absorbers: A

449 comparison on their performance with jet-absorbers and absorption columns,
450 Catalysts. 10 (2020) 1–14. https://doi.org/10.3390/catal10060653.

451 [27] S.J. Chung, I.S. Moon, An improved method of removal for high concentrations of
452 NO by electro-scrubbing process, Process Safety and Environmental Protection. 91
453 (2013) 153–158. https://doi.org/10.1016/j.psep.2012.05.010.

454 [28] M. Govindan, R. Adam Gopal, I.S. Moon, Efficient removal of gaseous
455 trichloroethylene by continuous feed electro-scrubbing using a new homogeneous
456 heterobimetallic electro-catalyst, Chemical Engineering Journal. 308 (2017) 1145–
457 1153. https://doi.org/10.1016/j.cej.2016.09.137.

458 [29] F. Escalona-Duran, M. Muñoz-Morales, K. de Freitas Araújo, C. Saez, P. Cañizares,
459 C. Martinez-Huitle, M. Rodrigo, Comparison of the performance of packed column
460 and jet electro-scrubbers for the removal of toluene, Journal of Environmental
461 Chemical Engineering. 9 (2021). https://doi.org/10.1016/j.jece.2021.106114.

462 [30] K. Chandrasekara Pillai, S.J. Chung, T. Raju, I.S. Moon, Experimental aspects of
463 combined NOx and SO2 removal from flue-gas mixture in an integrated wet
464 scrubber-electrochemical cell system, Chemosphere. 76 (2009) 657–664.
465 https://doi.org/10.1016/j.chemosphere.2009.04.013.

466 [31] S. Ardizzone, C.L. Bianchi, G. Cappelletti, A. Naldoni, C. Pirola, Photocatalytic
467 degradation of toluene in the gas phase: Relationship between surface species and
468 catalyst features, Environmental Science and Technology. 42 (2008) 6671–6676.
469 https://doi.org/10.1021/es8009327.

[32] J. Al-Sabahi, T. Bora, M. Al-Abri, J. Dutta, Efficient visible light photocatalysis of benzene, toluene, ethylbenzene and xylene (BTEX) in aqueous solutions using supported zinc oxide nanorods, PLoS ONE. 12 (2017) 1–16. https://doi.org/10.1371/journal.pone.0189276.

[33] A.N. Arias, R. de Mello, J. Lobato, A.J. Motheo, M.A. Rodrigo, Electrolytic removal of volatile organic compounds: Keys to understand the process, Journal of Electroanalytical Chemistry. 912 (2022) 116259. https://doi.org/10.1016/j.jelechem.2022.116259.

[34] T. Goto, M. Ogawa, Efficient photocatalytic oxidation of benzene to phenol by metal complex-clay/TiO2 hybrid photocatalyst, RSC Advances. 6 (2016) 23794–23797. https://doi.org/10.1039/c5ra25430b.

[35] I. Banga, A. Paul, A.U. Sardesai, S. Muthukumar, S. Prasad, M.A.T.H: Methanol vapor analytics through handheld sensing platform, Electrochimica Acta. 368 (2021) 137624. https://doi.org/10.1016/j.electacta.2020.137624.

[36] H. Cerfontain, Solubility of aromatic hydrocarbons in aqueous sulfuric acid, Recueil Des Travaux Chimiques Des Pays-Bas. 84 (1965) 491–502. https://doi.org/10.1002/recl.19650840414.

[37] M. Govindan, S.J. Chung, H.H. Moon, J.W. Jang, I.S. Moon, Development of a biphasic electroreactor with a wet scrubbing system for the removal of gaseous Benzene, ACS Combinatorial Science. 15 (2013) 439–446. https://doi.org/10.1021/co400046g.

[38] K.-W. Kim, M. Kuppuswamy, R.F. Savinell, Electrochemical oxidation of benzene at a glassy carbon electrode, Journal of Applied Electrochemistry. 30 (2000) 543–549.

[39] R.T.S. Oliveira, G.R. Salazar-Banda, M.C. Santos, M.L. Calegaro, D.W. Miwa, S.A.S. Machado, L.A. Avaca, Electrochemical oxidation of benzene on boron-doped diamond electrodes, Chemosphere. 66 (2007) 2152–2158. https://doi.org/10.1016/j.chemosphere.2006.09.024.

[40] I. Cesarino, V. Cesarino, F.C. Moraes, T.C.R. Ferreira, M.R.V. Lanza, L.H. Mascaro, S.A.S. Machado, Electrochemical degradation of benzene in natural water using silver nanoparticle-decorated carbon nanotubes, Materials Chemistry and Physics. 141 (2013) 304–309. https://doi.org/10.1016/j.matchemphys.2013.05.015.

[41] J. Schlauer, Absorption, 1. Fundamentals, in: Ullmann's Encyclopedia of Industrial Chemistry, Wiley-VCH Verlag GmbH & Co. KGaA, 2008. https://doi.org/10.1002/14356007.b03_08.pub2.

[42] A.G. Ramu, G. Muthuraman, P. Silambarasan, M. Il Shik, Sustainable generation of homogeneous Fe(VI) oxidant for the room temperature removal of gaseous N2O by electro-scrubbing process, Chemosphere. 272 (2021) 129497. https://doi.org/10.1016/j.chemosphere.2020.129497.

[43] M. Govindan, C. Sang-Joon, M. Il-Shik, Mineralization of Gaseous Acetaldehyde by Electrochemically Generated Co(III) in H2SO4 with Wet Scrubber Combinatorial System, ACS Combinatorial Science. 14 (2012) 359–365.

[44] M. Govindan, I.S. Moon, A single catalyst of aqueous CoIII for deodorization of mixture odor gases: A development and reaction pathway study at electro-scrubbing process, Journal of Hazardous Materials. 260 (2013) 1064–1072. https://doi.org/10.1016/j.jhazmat.2013.06.055.

529

530 **Appendix I: Supplementary material**

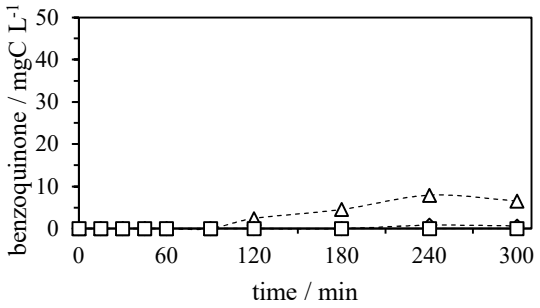

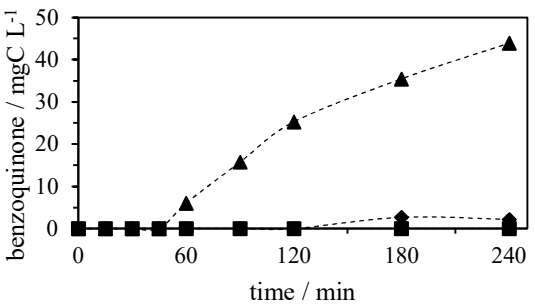

531

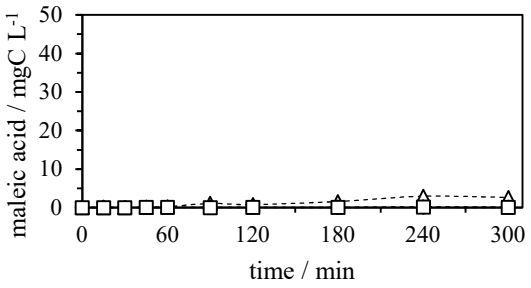

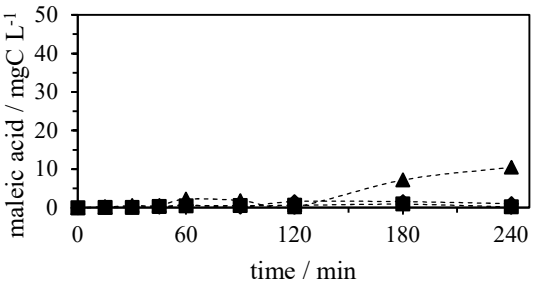

532

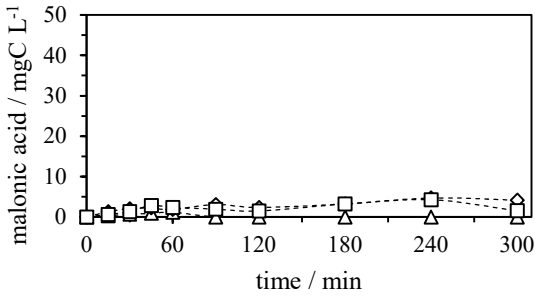

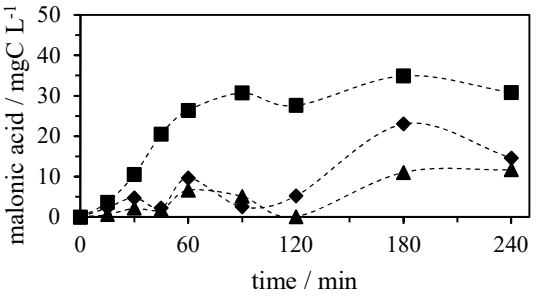

533

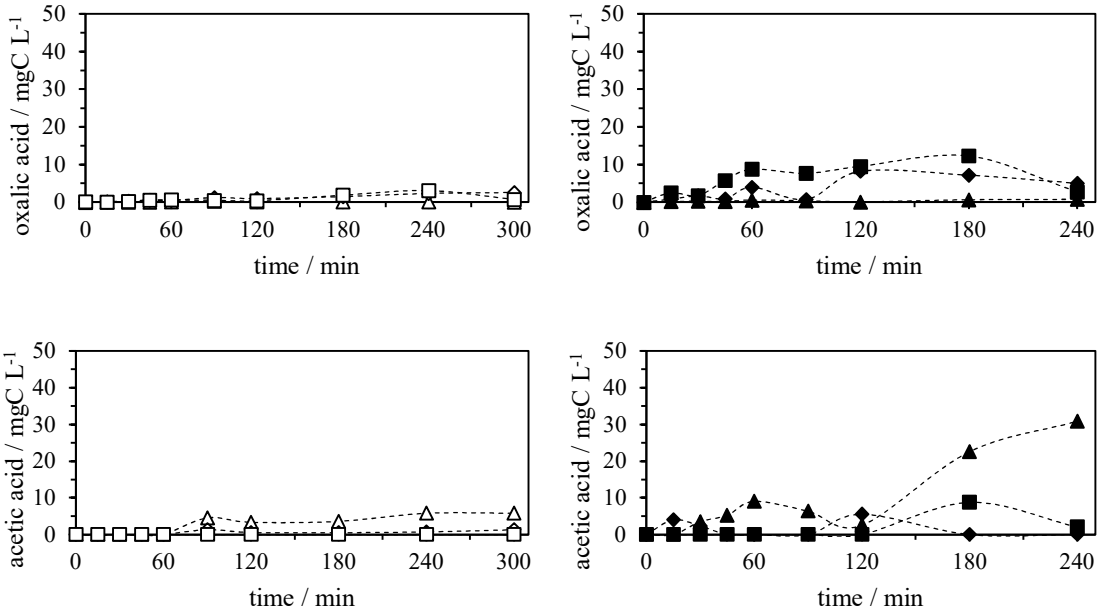

Figure S1. Time evolution of each intermediates compounds identified in the liquid phase at different gaseous flow of 1.5 (white) and 6 (black) L h^{-1} in electro-absorption processes at 10 (triangle), 50 (rhombus) and 100 (square) mA cm^{-2}.

Table S1. Mass of benzene (mgC) retained on the active carbon after the electro-absorption process and the percentage of each value in relation to the total mass entering the system.

	Current density (mA cm^{-2})			
Inlet gas flow (L h^{-1})	0	10	50	100
1.5	708.52 (57%)	355.88 (29%)	246.23 (19%)	137.37 (11%)
6.0	3208.86 (68%)	2858.70 (63%)	2463.70 (52%)	1940.83 (44%)